

Supporting information

High-Yielding Preparation of Hierarchically Branched Carbon Nanotubes Derived from Zeolitic Imidazolate Frameworks for Enhanced Electrochemical K⁺ Storage

Dongbo Yu^{a,b,c}, Fei Wang^a, Jie Wang^a, Qingliang Gao^a, Jiaqin Liu^{b,c,}, Gang Qian^{d,*},
Yong Zhang^{a,b,c}, Yucheng Wu^{a,b,c}, Jiewu Cui^{a,b,c,*}*

^a School of Materials Science and Engineering, Hefei University of Technology,
Hefei 230009, Anhui, China

^b China International S&T Cooperation Base for Advanced Energy and
Environmental Materials & Anhui Provincial International S&T Cooperation Base for
Advanced Energy Materials, Hefei 230009, Anhui, China

^c Key Laboratory of Advanced Functional Materials and Devices of Anhui Province,
Hefei 230009, Anhui, China

^d Instrumental Analysis Center, Hefei University of Technology, Hefei 230009, Anhui,
China

Email Address: jqliu@hfut.edu.cn (Jiaqin Liu); qiangang.qg@163.com (Gang Qian);
jwcui@hfut.edu.cn (Jiewu Cui);

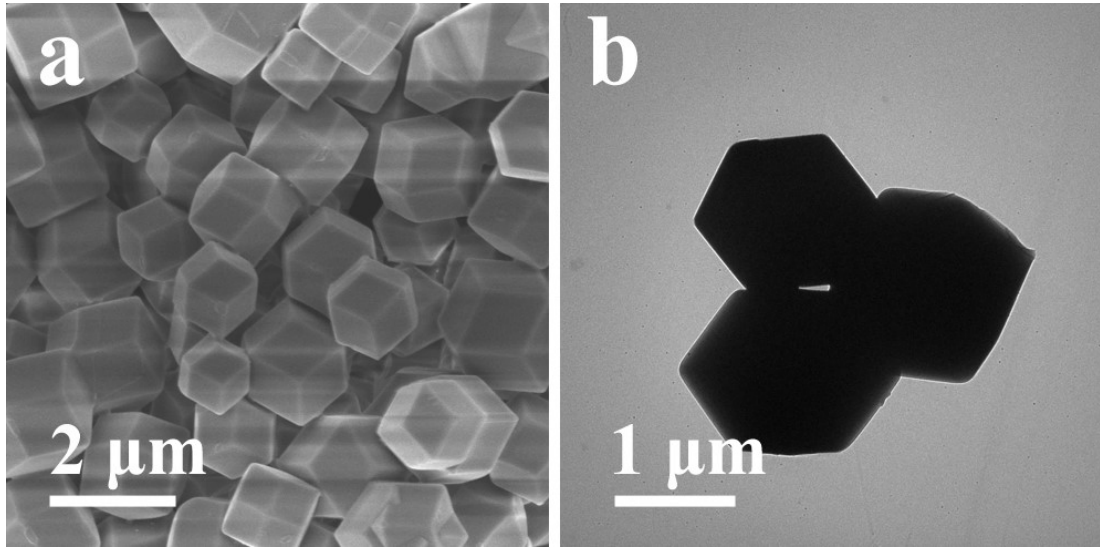


Fig. S1 SEM (a) and TEM (b) images of ZnCo-ZIF particles.

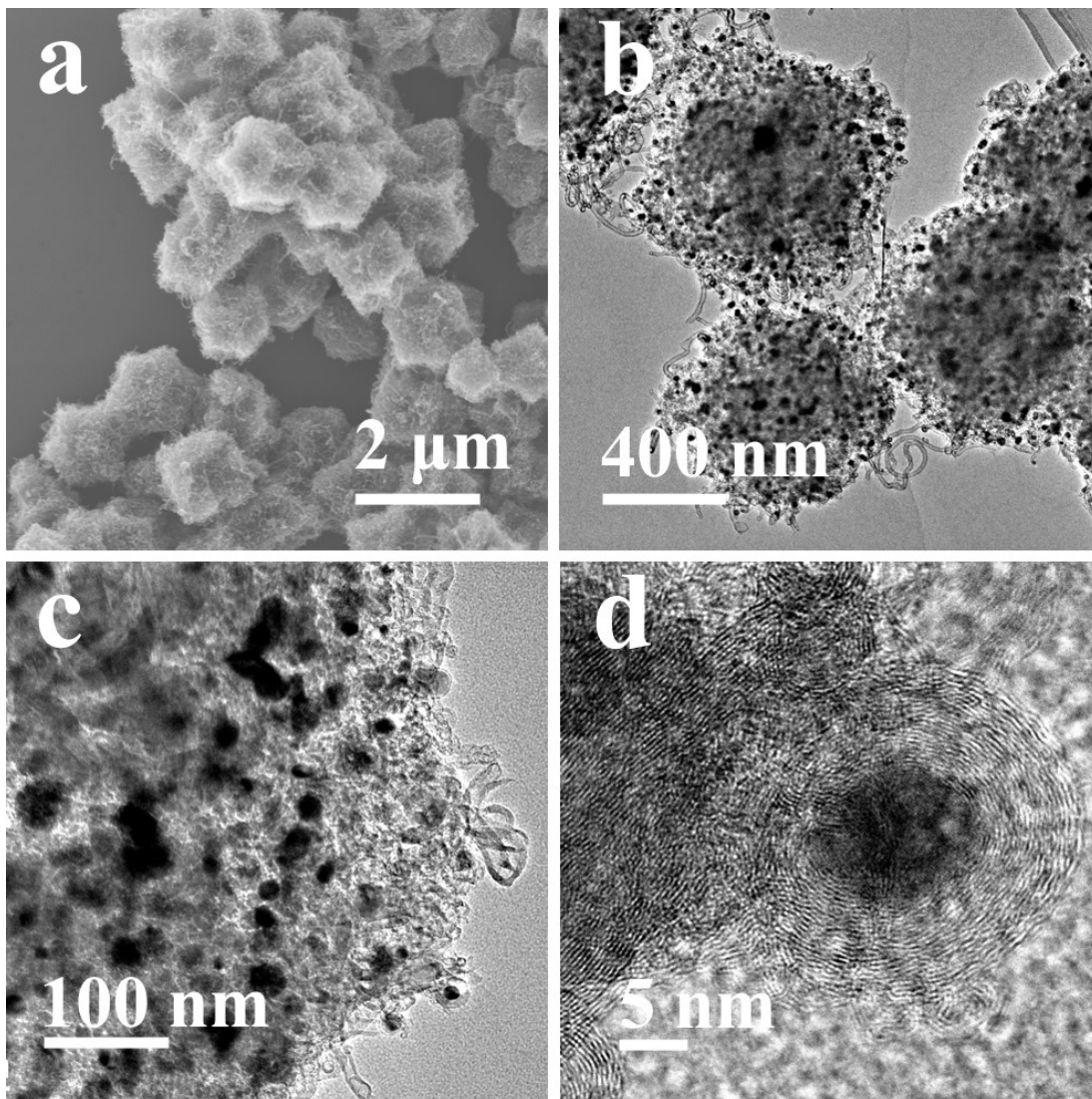


Fig. S2 SEM (a), TEM (b, c) and HRTEM (d) images of ZnCo-ZIF particle-derived urchin-like carbon (u-CPs).

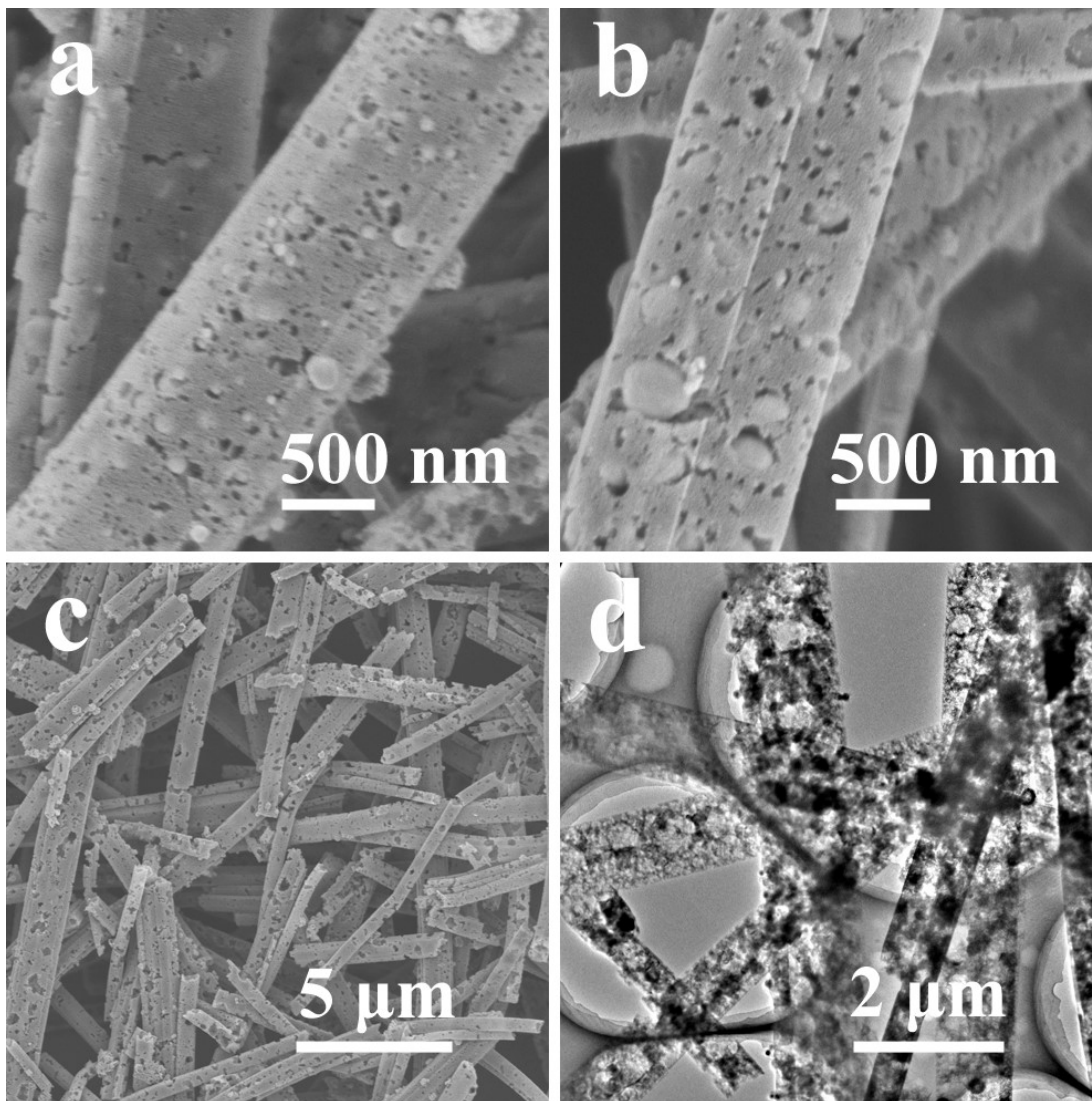


Fig. S3 SEM images of ZnCo-BTC NW after carbonization treatment but before nitrate acid etching (a, b); SEM (c) and TEM (d) images of ZnCo-BTC NW-derived carbon nanowires (CNWs) after nitrate acid etching.

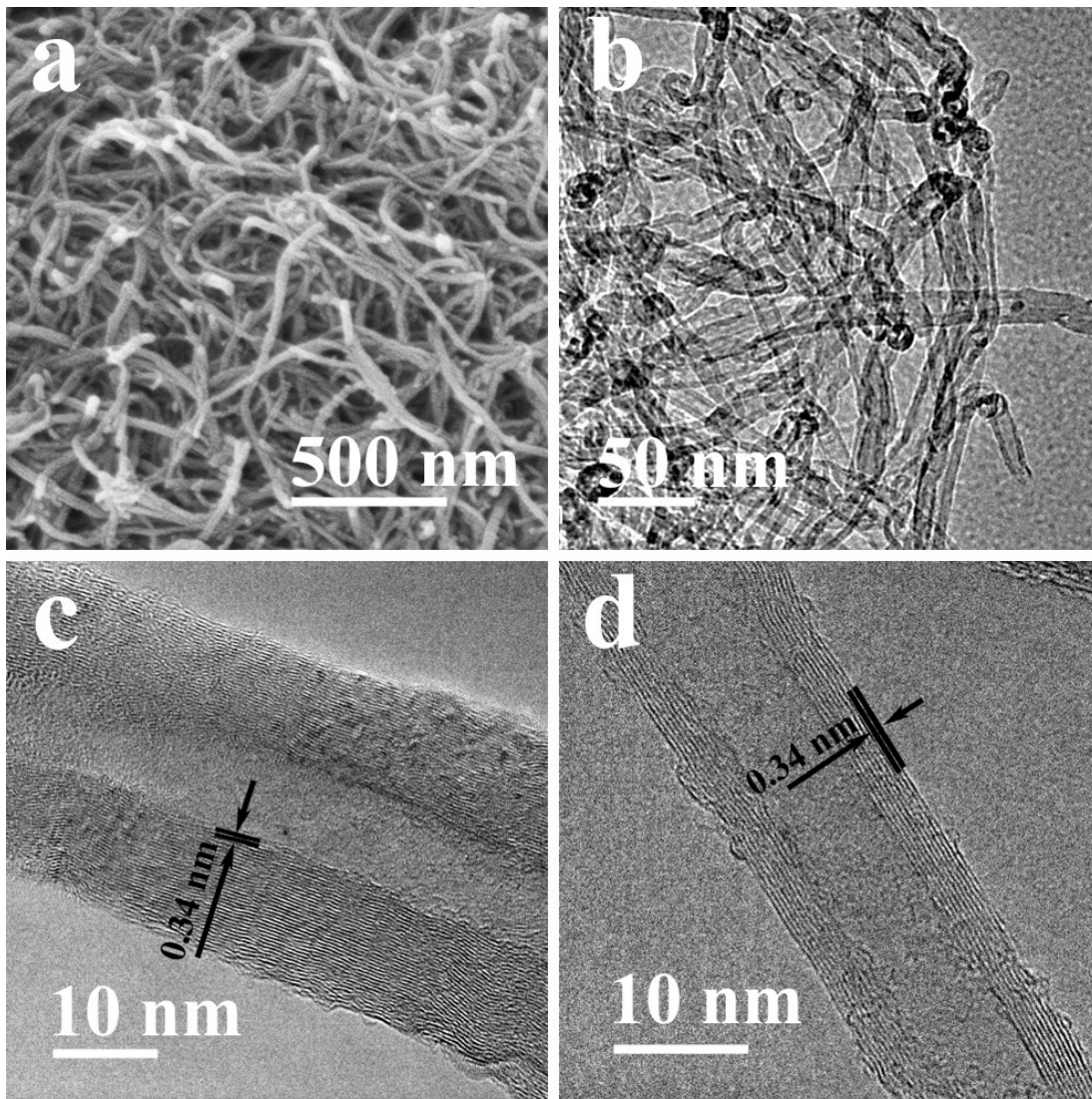


Fig. S4 SEM (a), TEM (b) and HRTEM (c, d) images of commercial carbon nanotubes (c-CNTs).

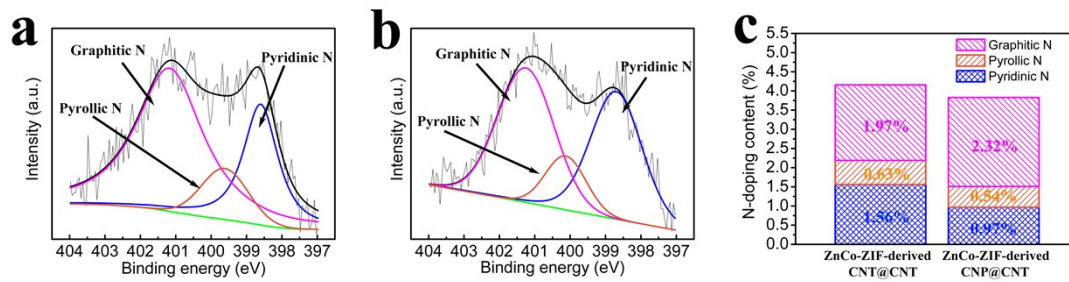


Fig. S5 The high-resolution XPS spectra of N 1s of u-CPs (a) and br-CNTs (b); the specific N-doping contents of u-CPs and br-CNTs (c).

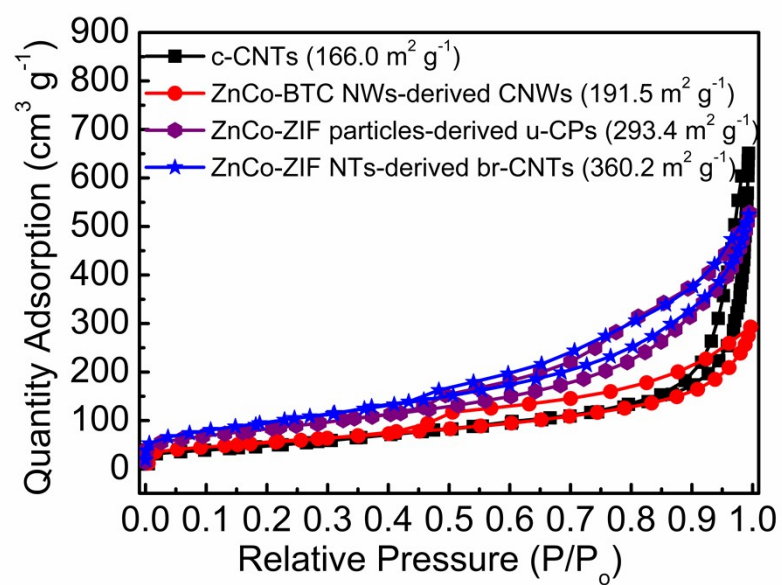


Fig. S6 Nitrogen adsorption-desorption isotherms of c-CNTs (a), CNWs (b), u-CPs (c) and br-CNTs (d).

Table S1 Percentage of pores in different size range for c-CNTs, CNWs, u-CPs and br-CNTs.

Materials	≤ 2 nm	2 ~ 5 nm	5 ~ 10 nm	10 ~ 50 nm	> 50 nm
c-CNTs	0.44%	11.14%	6.79%	22.26%	59.37%
CNWs	2.14%	22.78%	15.50%	33.04%	26.54%
u-CPs	1.42%	18.01%	18.47%	39.67%	22.43%
br-CNTs	1.19%	22.84%	19.79%	36.89%	19.30%

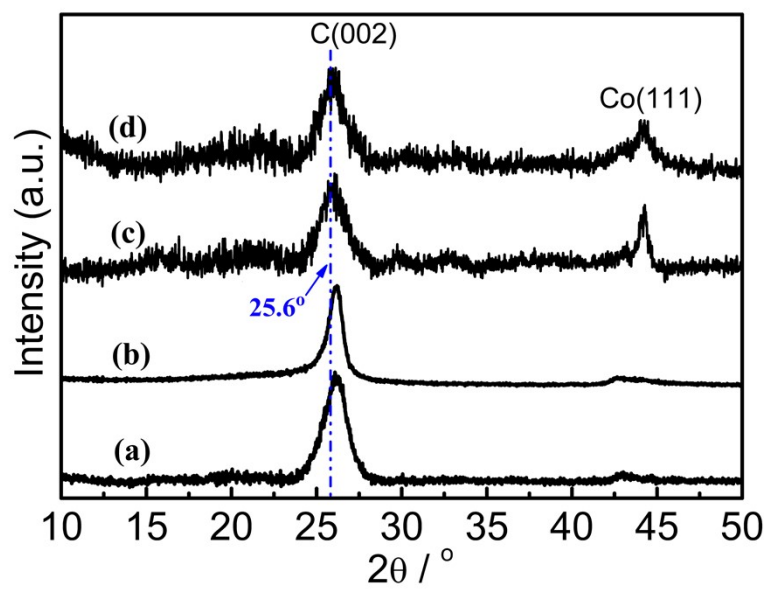


Fig. S7 XRD patterns of c-CNTs (a), CNWs (b), u-CPs (c) and br-CNTs (d).

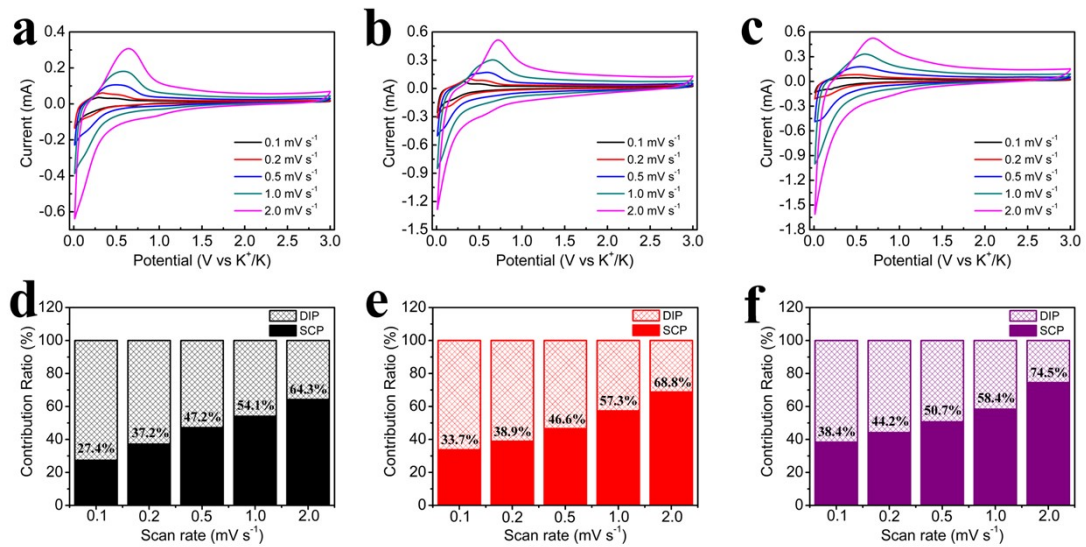


Fig. S8 CV plots of c-CNTs (a), CNWs (b) and u-CPs (c) at different scan rates; the corresponding contribution ratio of DIP and SCP versus scan rate calculated from CV plots of c-CNTs (d), CNWs (e) and u-CPs (f).

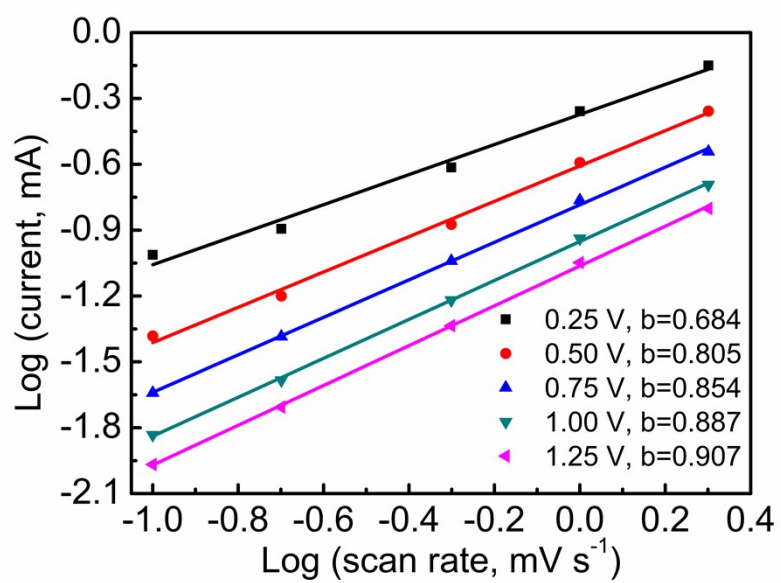


Fig. S9 The linear relationships between the logarithm current and logarithm scan rate calculated from CV curves of br-CNTs in Fig. 3d.

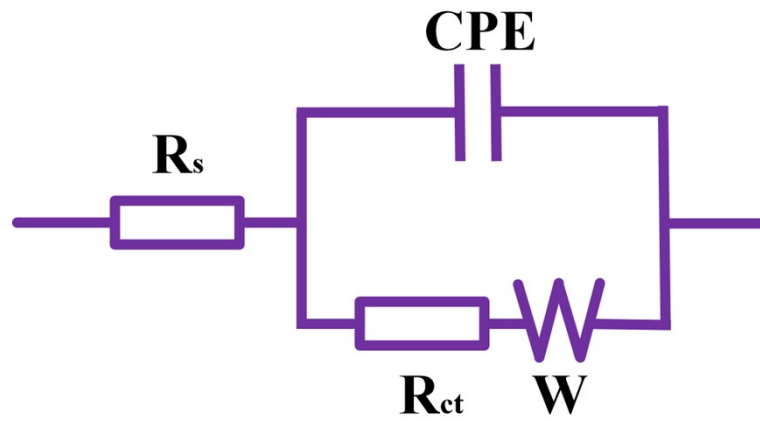


Fig. S10 The fitting equivalent circuit of Nyquist plots in Fig. 3f, where R_s , R_{ct} , CPE and W corresponded to series resistance, charge transfer resistance, constant phase element and Warburg impedance, respectively.

Table S2 R_s , R_{ct} and CPE values fitted from Nyquist plots according to the equivalent circuit in Figure S10.

Materials	R_s (Ω)	R_{ct} (Ω)	CPE (F)
c-CNTs	17.01	6043	0.000020068
CNWs	8.087	4370	0.000040941
u-CPs	7.317	3249	0.000048539
br-CNTs	6.667	2255	0.000029429

Table S3 K⁺ storage properties of MOF-derived materials in recent literature.

Materials	Specific Capacity	Rate Capability	Cycling Stability	References
Cu-MOF-derived hollow porous carbon	370 mAh g ⁻¹ at 0.1 A g ⁻¹	190 mAh g ⁻¹ at 1 A g ⁻¹	100 % after 3000 cycles at 1 A g ⁻¹	<i>Small</i> , 2021 , 17, 2100538
Mn-BDC MOFs-derived carbon	266.4 mAh g ⁻¹ at 0.05 A g ⁻¹	93 mAh g ⁻¹ at 2 A g ⁻¹ ; 57.2 mAh g ⁻¹ at 5 A g ⁻¹	100% after 1000 cycles at 0.2 A g ⁻¹	<i>Adv. Funct. Mater.</i> , 2020 , 30, 2006561
Cu-MOF-derived N-doped porous carbon nanosheets	276 mAh g ⁻¹ at 50 mA g ⁻¹	184 mAh g ⁻¹ at 1 A g ⁻¹ ; 157 mAh g ⁻¹ at 2 A g ⁻¹	94.5% after 6000 cycles at 1 A g ⁻¹	<i>Angew. Chem. Int. Ed.</i> , 2020 , 59, 19460
LDH/ZIF-67-derived honeycomb-like carbon	367.1 mAh g ⁻¹ at 0.05 A g ⁻¹	162.7 mAh g ⁻¹ at 2 A g ⁻¹	67.9% after 200 cycles at 1 A g ⁻¹	<i>Chem. Eng. J.</i> , 2020 , 384: 123328
Macroporous ZIF-8 single crystal-derived N-doped carbon	345 mAh g ⁻¹ at 0.1 A g ⁻¹	180 mAh g ⁻¹ at 1 A g ⁻¹ ; 94 mAh g ⁻¹ at 10 A g ⁻¹	105.4% after 12000 cycles at 2 A g ⁻¹	<i>Nano Lett.</i> , 2019 , 19, 4965
MIL-100-derived S/N co-doped thin carbon	320 mAh g ⁻¹ at 50 mA g ⁻¹	91.2 mAh g ⁻¹ at 2 A g ⁻¹	71.3% after 900 cycles at 2 A g ⁻¹	<i>Adv. Mater.</i> , 2019 , 31, 1805430
ZIF-8-derived N-doped meso-macro porous carbon	312 mAh g ⁻¹ at 0.2 C	117 mAh g ⁻¹ at 21 C	93.2 % after 2000 cycles at 2 A g ⁻¹	<i>J. Mater. Chem. A</i> , 2019 , 7, 21966
Cu-BTC-derived N/O co-doped carbon	354 mAh g ⁻¹ at 50 mA g ⁻¹	110 mAh g ⁻¹ at 1 A g ⁻¹	90.9% after 1300 cycles at 1 A g ⁻¹	<i>J. Mater. Chem. A</i> , 2019 , 7, 12317
Co-HMT-derived carbon nanosheets	311 mAh g ⁻¹ at 0.1 A g ⁻¹	168 mAh g ⁻¹ at 2 A g ⁻¹	96% after 10000 cycles at 5 A g ⁻¹	<i>J. Mater. Chem. A</i> , 2019 , 7, 18499
MIL-101-derived N/O-doped hard carbon	365 mAh g ⁻¹ at 25 mA g ⁻¹	118 mAh g ⁻¹ at 3 A g ⁻¹	69.5% after 1100 cycles at 1.05 A g ⁻¹	<i>Adv. Mater.</i> , 2018 , 30, 1700104
ZIF-67-derived high pyridine N-doped porous carbon	359.6 mAh g ⁻¹ at 0.2 A g ⁻¹	207.8 mAh g ⁻¹ at 2 A g ⁻¹	≈ 71% after 2000 cycles at 0.5 A g ⁻¹	<i>J. Mater. Chem. A</i> , 2018 , 6, 17959
ZIF-67-derived porous carbon	587.6 mAh g ⁻¹ at 50 mA g ⁻¹	186.2 mAh g ⁻¹ at 2 A g ⁻¹	39.4% after 2000 cycles at 0.5 A g ⁻¹	<i>J. Mater. Chem. A</i> , 2018 , 6, 17959
Zn-MOF@Co-MOF nanosheet-derived	310 mA h g ⁻¹ at 100 mA g ⁻¹	170 mAh g ⁻¹ at 2 A g ⁻¹ ; 120 mAh g ⁻¹ at 5 A g ⁻¹	89.3% after 5200 cycles at 1 A g ⁻¹	<i>J. Mater. Chem. A</i> , 2019 , 7, 19929

carbon				
Al-MIL-NH₂ nanorod-derived N-doped carbon	305 mA h g ⁻¹ at 100 mA g ⁻¹	202 mAh g ⁻¹ at 1 A g ⁻¹ ; 162 mAh g ⁻¹ at 6 A g ⁻¹	~ 100% after 500 cycles at 6 A g ⁻¹	<i>Small</i> , 2021 , 17, 2100135
MIL-88A-derived S-doped carbon	358.4 mAh g ⁻¹ at 50 mA g ⁻¹	192.6 mAh g ⁻¹ at 2 A g ⁻¹	90.9% after 700 cycles at 1 A g ⁻¹	<i>ACS Appl. Energy Mater.</i> , 2021 , 4, 2282
ZIF-67-derived N-doped carbon nanotubes	254.7 mAh g ⁻¹ at 50 mA g ⁻¹	180 mAh g ⁻¹ at 0.5 A g ⁻¹ ; 131 mAh g ⁻¹ at 2 A g ⁻¹	77.86% after 500 cycles at 2 A g ⁻¹	<i>ChemSusChem</i> , 2018 , 11, 202
Bi-MOF-derived carbon film@carbon nanorods@Bi nanoparticle	425 mAh g ⁻¹ at 0.1 A g ⁻¹	140 mAh g ⁻¹ at 1 A g ⁻¹	74.8% after 700 cycles at 1 A g ⁻¹	<i>ACS Appl. Energy Mater.</i> , 2019 , 11, 22474
ZIF-67-derived open ZnSe/C nanocages	318 mAh g ⁻¹ at 0.05 A g ⁻¹	205 mAh g ⁻¹ at 0.5 A g ⁻¹	92.19% after 400 cycles at 0.5 A g ⁻¹	<i>J. Mater. Chem. A</i> , 2020 , 8, 779
ZIF-8@ZIF-67-derived N-doped CoP/C polyhedron	310 mAh g ⁻¹ at 0.1 A g ⁻¹	220 mAh g ⁻¹ at 1A g ⁻¹	70% after 800 cycles at 0.5 A g ⁻¹	<i>Small</i> , 2020 , 16, 1906566
ZIF-67-derived N-doped carbon/CoSe nanocubes	388.7 mAh g ⁻¹ at 0.1 A g ⁻¹	365.9 mAh g ⁻¹ at 2 A g ⁻¹	84.6% after 500 cycles at 2 A g ⁻¹	<i>J. Colloid Interf. Sci.</i> , 2021 , 604, 157
ZIF-67-derived Co_{0.85}Se@C nanofibers	364 mAh g ⁻¹ at 0.2 A g ⁻¹	303 mAh g ⁻¹ at 2 A g ⁻¹	87.42% after 400 cycles at 1 A g ⁻¹	<i>Energy Storage Mater.</i> , 2020 , 24, 167
ZIF-67-derived CoP/reduced graphene oxide	360 mAh g ⁻¹ at 0.1 A g ⁻¹	189 mAh g ⁻¹ at 1 A g ⁻¹ ; 155 mAh g ⁻¹ at 2 A g ⁻¹	93.65% after 2800 cycles at 1 A g ⁻¹	<i>J. Colloid Interf. Sci.</i> , 2021 , 604, 319
ZnCo-ZIF-derived branched carbon nanotubes	450.2 mAh g ⁻¹ at 0.05 A g ⁻¹ ; 348.0 mAh g ⁻¹ at 0.1 A g ⁻¹	199.5 mAh g ⁻¹ at 1 A g ⁻¹ ; 147.2 mAh g ⁻¹ at 2 A g ⁻¹	91.6%, 86.9% and 84.5% after 500, 1000 and 1300 cycles at 2 A g ⁻¹	This work

Table S4 K⁺ storage properties of other carbon materials in recent literature.

Materials	Specific Capacity	Rate Capability	Cycling Stability	References
N-doped carbon spheres	363.7 mAh g ⁻¹ at 0.05 A g ⁻¹	107.9 mAh g ⁻¹ at 5 A g ⁻¹	56.8 % after 3600 cycles at 1 A g ⁻¹	<i>Nano-Micro Lett.</i> , 2021 , 13, 174
Gelatin-derived carbon	132 mAh g ⁻¹ at 0.1 A g ⁻¹	53.8 mAh g ⁻¹ at 1 A g ⁻¹	89.3 % after 300 cycles at 0.2 A g ⁻¹	<i>Carbon</i> , 2021 , 178, 775-782
O-rich carbon nanosheets	392 mAh g ⁻¹ at 0.05 A g ⁻¹	174 mAh g ⁻¹ at 2 A g ⁻¹	≈ 128.5 % after 2500 cycles at 2 A g ⁻¹	<i>Nanoscale</i> , 2021 , 13, 2389
P/N co-doped porous carbon monoliths	437 mA h g ⁻¹ at 0.05 A g ⁻¹	205 mA h g ⁻¹ at 2 A g ⁻¹	84.2 % after 3000 cycles at 1 A g ⁻¹	<i>ACS Nano</i> , 2020 , 14, 14057
N/O dual-doped hard carbon	439.1 mAh g ⁻¹ at 100 mA g ⁻¹	254.4 mAh g ⁻¹ at 1 A g ⁻¹ ; 223.4 mAh g ⁻¹ at 2 A g ⁻¹	74.5% after 5000 cycles at 1 A g ⁻¹	<i>Adv. Sci.</i> , 2020 , 7, 1902547
N/S dual-doped graphitic hollow architectures	≈ 220 mAh g ⁻¹ at 500 mA g ⁻¹	192 mAh g ⁻¹ at 1 A g ⁻¹ ; 155 mAh g ⁻¹ at 2 A g ⁻¹	90.2% after 5000 cycles at 5 A g ⁻¹	<i>Adv. Energy Mater.</i> , 2020 , 10, 2001161
Polyaniline-co-poly pyrrole-derived N-doped carbon	423 mAh g ⁻¹ at 50 mA g ⁻¹	195 mAh g ⁻¹ at 1 A g ⁻¹ ; 148 mAh g ⁻¹ at 2 A g ⁻¹	93.8% after 660 cycles at 0.2 A g ⁻¹	<i>Angew. Chem. Int. Ed.</i> , 2020 , 59, 4448
Superabsorbent polymers-derived porous carbon	291.9 mAh g ⁻¹ at 50 mA g ⁻¹	151.4 mAh g ⁻¹ at 1 A g ⁻¹ ; 136.7 mAh g ⁻¹ at 2 A g ⁻¹	106.8% after 2000 cycles at 1 A g ⁻¹	<i>J. Power Sources</i> , 2020 , 451, 227727
Nitrogen-doped turbostratic carbon	518 mAh g ⁻¹ at 50 mA g ⁻¹	212 mAh g ⁻¹ at 2 A g ⁻¹ ; 119 mAh g ⁻¹ at 5 A g ⁻¹	93.1% after 500 cycles at 1 A g ⁻¹	<i>Adv. Mater.</i> , 2020 , 32, 2000732
Crustacean-derived porous hard carbon nanobelts	468 mAh g ⁻¹ at 50 mA g ⁻¹	235 mAh g ⁻¹ at 1.6 A g ⁻¹	≈ 100% after 1600 cycles at 1 A g ⁻¹	<i>Nano Energy</i> , 2020 , 77, 105018
Silicon carbide - derived carbon	289.9 mAh g ⁻¹ at 100 mA g ⁻¹	197.3 mAh g ⁻¹ at 1 A g ⁻¹	89.3% after 1000 cycles at 1 A g ⁻¹	<i>Adv. Funct. Mater.</i> , 2020 , 30, 2004348
Pitch-derived carbon	290 mAh g ⁻¹ at 0.1 A g ⁻¹	146 mAh g ⁻¹ at 2 A g ⁻¹	80 % after 2000 cycles at 1 A g ⁻¹	<i>Carbon</i> , 2021 , 176, 383

Acetonitrile-derived porous carbon	271 mAh g ⁻¹ at 50 mA g ⁻¹	135 mAh g ⁻¹ at 1 A g ⁻¹ ; 98 mAh g ⁻¹ at 5 A g ⁻¹	82% after 600 cycles at 0.1 A g ⁻¹	<i>J. Power Sources</i> , 2020 , 466, 228303
N/F dual doped soft carbon nanofibers	262 mAh g ⁻¹ at 0.1 A g ⁻¹	146 mAh g ⁻¹ at 5 A g ⁻¹	78.5 % after 1000 cycles at 1 A g ⁻¹	<i>Small</i> , 2021 , 17, 2101576
Ni-EDTA-derived N-doped carbon	369 mAh g ⁻¹ at 50 mA g ⁻¹	152 mAh g ⁻¹ at 1 A g ⁻¹ ; 123 mAh g ⁻¹ at 2 A g ⁻¹	82% after 200 cycles at 0.2 A g ⁻¹	<i>Adv. Funct. Mater.</i> , 2019 , 29, 1903641
Gelatin-derived carbon	132 mAh g ⁻¹ at 0.1 A g ⁻¹	53.8 mAh g ⁻¹ at 1 A g ⁻¹	89.3 % after 300 cycles at 0.2 A g ⁻¹	<i>Carbon</i> , 2021 , 178, 775
Amorphous ordered mesoporous carbon	286.4 mAh g ⁻¹ at 50 mA g ⁻¹	144.2 mAh g ⁻¹ at 1 A g ⁻¹	101.6% after 1000 cycles at 1 A g ⁻¹	<i>Adv. Energy Mater.</i> , 2018 , 8, 1701648
Spent asphalt-derived mesoporous carbon	289 mAh g ⁻¹ at 0.1 A g ⁻¹	197.3 mAh g ⁻¹ at 1 A g ⁻¹	89.3 % after 1000 cycles at 1 A g ⁻¹	<i>Adv. Funct. Mater.</i> , 2020 , 30, 2004348
Soybeans-derived hard carbon	175 mAh g ⁻¹ at 0.05 A g ⁻¹	70 mAh g ⁻¹ at 0.8 A g ⁻¹	≈ 100 % after 900 cycles at 0.05 A g ⁻¹	<i>J. Power Sources</i> , 2020 , 463, 228172
PPy-derived N-doped carbon nanofiber	238 mAh g ⁻¹ at 100 mA g ⁻¹	172 mAh g ⁻¹ at 1 A g ⁻¹ ; 153 mAh g ⁻¹ at 2 A g ⁻¹	95.3% after 2000 cycles at 1 A g ⁻¹	<i>Nat. Commun.</i> , 2018 , 9, 1720.
Pitch-derived soft carbon	461.2 mAh g ⁻¹ at 0.1 A g ⁻¹	224 mAh g ⁻¹ at 1 A g ⁻¹	70 % after 1000 cycles at 1 A g ⁻¹	<i>Carbon</i> , 2019 , 155, 601
Sycamore leaves-derived carbon microtube	432 mAh g ⁻¹ at 0.2 A g ⁻¹	273.6 mAh g ⁻¹ at 1 A g ⁻¹	92.48 % after 100 cycles at 0.5 A g ⁻¹	<i>J. Mater. Chem. A</i> , 2019 , 7, 25845
Hierarchically N-doped porous carbon	381.7 mAh g ⁻¹ at 0.05 A g ⁻¹	185.0 mAh g ⁻¹ at 10 A g ⁻¹	86.0% after 1000 cycles at 2.0 A g ⁻¹	<i>Adv. Energy Mater.</i> , 2018 , 8, 1802386
ZnCo-ZIF-derived branched carbon nanotubes	450.2 mAh g ⁻¹ at 0.05 A g ⁻¹ ; 348.0 mAh g ⁻¹ at 0.1 A g ⁻¹	199.5 mAh g ⁻¹ at 1 A g ⁻¹ ; 147.2 mAh g ⁻¹ at 2 A g ⁻¹	91.6%, 86.9% and 84.5% after 500, 1000 and 1300 cycles at 2 A g ⁻¹	This work